Journal of Building Pathology and Rehabilitation (2021) 6:29
https://doi.org/10.1007/s41024-021-00126-1

RESEARCH ARTICLE

Analytical model for bond–slip behavior of the anchorage of deformed bars in reinforced concrete members subjected to bending

Maruful Hasan Mazumder[1] · **Raymond Ian Gilbert**[2] · **Zhen- Tian Chang**[2]

Received: 22 July 2021 / Revised: 22 July 2021 / Accepted: 28 August 2021 / Published online: 8 September 2021

Abstract

The distribution of bond stresses along the anchorage of a reinforcing bar in concrete plays a key role in controlling the load transfer and inelastic deformation of a Reinforced Concrete (RC) member under load. The typical bond stress–slip relationships specified in the model codes are given as average 'local bond stress' versus 'local slip' relationships which may be taken as statistically acceptable to represent bond–slip behavior in RC specimens with short anchorage lengths. This paper demonstrates the use of a viable analytical procedure for calibration of bond–slip relationships of the anchorage of deformed bars in RC members subjected to bending. The analytical modelling of the bond–slip relationship is based on observations of load-deflection behavior in laboratory experiments of full-scale RC specimens designed with relatively long end development of anchored bars beyond a critical section. The calibrated bond–slip relationships for selected anchorage specimens have been used to develop a modified model of peak local bond stress for splitting type bond failure. The model proposed in this paper takes into account the effect of variations of anchorage length on the bond–slip behavior, in addition to the effects of bar diameters, concrete cover and concrete strength that are typically taken into account in the model codes.

Keywords Anchorage · Anchorage length · Bond stress · Bond failure · Reinforced concrete

1 Introduction

The distribution of bond stress along the anchorage of reinforcing bars in concrete is of crucial importance since it controls the load transfer and the inelastic deformation of a Reinforced Concrete (RC) member under load. The typical bond stress–slip relationships specified in the model codes (e.g., in FIB Model Code 2010 [1]) are formulated based on the assumption that under well-defined conditions, there exists an average 'local bond stress' versus 'local slip' relationship that is statistically acceptable for short anchorage lengths. The specifications in different codes of practices (e.g., in [2–5]) for determining the development length or lapped splice length of anchored bars are also based on data mostly obtained from small-scale RC "pull-out" test specimens with relatively short embedment lengths of bars. Local bond–slip models are mainly based on test data such as that obtained from the RILEM pull-out test [6, 7] with a short anchorage length typically five times the bar diameter and with a relatively thick concrete cover equal to 4.5 times the bar diameter [8, 9]. Although the FIB Model Code 2010 [1] has extended its local bond–slip model to cover splitting failure modes, bond–slip models for deformed bars have historically been derived first for well-confined conditions in which concrete cover of sufficient thickness ensures a pull-out failure mode in which the bar pulls out of the concrete leaving a smooth hole and without splitting the cover [9]. At the ultimate state of bond failure, the pull-out specimens with short anchorage length typically develop nearly uniform bond stress distributions at the bar concrete interface. Therefore, the scope of application of these bond–slip relationships for modelling typically longer anchorages of reinforcement in full-scale RC members is questionable [10].

✉ Maruful Hasan Mazumder
maruf320@yahoo.com; mhasandee@cuet.ac.bd

Raymond Ian Gilbert
i.gilbert@unsw.edu.au

Zhen- Tian Chang
z.chang@unsw.edu.au

[1] Department of Disaster Engineering and Management, Chittagong University of Engineering and Technology, Chittagong 4349, Bangladesh

[2] School of Civil and Environmental Engineering, University of New South Wales, Sydney, NSW 2052, Australia

Bond–slip phenomenon significantly affects the structural behavior and efficiency of different sub-elements in a RC frame, including column, foundation, interior and exterior beam–column joint [11]. It also affects the crack patterns and failure modes in RC beams and slabs [11]. The validation of the existing analytical models of bond–slip were mostly performed on small-size specimens, where only the elementary features of the models were tested [12, 13]. In many cases when RC structures are considered, one of the most used approaches of modelling is to consider a no slip relationship between steel and concrete, i.e., perfect bond [12, 14]. Although the assumption of perfect bond between the concrete and reinforcing bar is often a sufficient assumption when modelling the ultimate behavior of a large RC structure, it is not of course appropriate when modelling bond or anchorage failure in RC members [15].

The bar–concrete interface along the anchorage is treated as a continuum in the formulation of a typical analytical bond–slip model. However, the random development of cracks may affect the bond stresses [16, 17]. Existing models ignore such extreme variations or discontinuities in local bond stresses and the local slips that may occur at or in the vicinity of the flexural cracks. As the reinforcement–concrete bond directly influences the evolutions of cracks, implementation of the no slip relation may produce impractical model outputs in numerical simulations of practical situations of RC members under load (e.g., [12, 15, 18–20]). Notwithstanding, the bond–slip models proposed by different researchers vary widely depending on the particular anchorage type being modeled (e.g., [1, 21–24]) or depending on the particular type and geometry of a structure and its response under variable loading conditions (e.g., [25]).

Therefore, a reasonable representation of the highly nonlinear bond stress–slip relationships usually observed in laboratory experiments is required to obtain reliable outputs especially when modelling the behavior of full-scale RC specimens under overload. Based on observations of laboratory test results of the two types of anchorage length RC specimens reported elsewhere by Gilbert et al. [16, 26] and Mazumder et al. [27–30], it was evident that the average ultimate bond stresses along an anchored bar varied significantly depending on the variations of the anchorage lengths and the bar diameters in the specimens. In practical cases of longer anchorage lengths provided in RC members, average bond strength generally decreases with increasing anchorage length [8, 16, 31]. One of the possible reasons for the variations was ascribed to the presence of flexural cracks along the anchorage zone of full-scale RC specimens [10, 16, 17]. Therefore, it is reasonable to consider that the local bond–slip relationships to be used for analytical or numerical modelling in RC specimens should not only depend on the bar diameters but also on the anchorage lengths provided in the specimens.

This paper discusses the test results from a few selected anchorage length RC slab specimens that were tested by the authors under three-point bending action. The load-deflection behavior of the RC test specimens was observed during the experiment up to the point of anchorage failure. A simple but viable analytical model of bond–slip proposed by Yankelevsky [32] was used and a systematic procedure of calibration of bond–slip models was performed using the test results [31]. The efficacy and validation of the recalibrated analytical model of bond–slip relationships [31] for finite element (FE) modelling of full-scale RC anchorage length specimens has been reported by Mazumder and Gilbert [15]. This paper aims at presenting the detailed mathematical formulations and solutions of the analytical model of the local bond–slip relationships and also discusses the detailed procedure for verifying a local bond–slip relationship that is consistent with the experimental test data. The application of calibrated bond–slip relationships for the specimens is extended further to develop a modified model of peak local bond stress for splitting type bond failure.

2 Experimental program

A series of tests on 18 full-scale anchorage length RC slab specimens had been fabricated and tested under static, cyclic and sustained loads and the test results have been reported elsewhere [16, 17, 26–30]. The discussion in this paper concerns the test results of seven selected anchorage length RC slab specimens that were tested under monotonic static loads. The RC slab specimens were of equal dimensions each being 2000 mm long, 600 mm wide and 200 mm deep. The two supports of the slab were at 1200 mm distance and the specimens overhung at one end by 700 mm. The location of the applied line load P was at a distance 600 mm past Support 1, as shown in Fig. 1a. Among the four reinforcement bars at the top of the specimen, the external two bars were discontinued with a 180° cog past Support 1. For the two middle bars resisting bending action in the cantilever, the bond between the bars and the concrete was discontinued at a distance l_d (anchorage length) past Support 1 by encasing each middle bar in a plastic sleeve through to the other end of the specimen. For testing with a convenient experimental set-up, the specimen was inverted to keep the anchored bars located at the bottom of the specimen (see Fig. 1c). A monotonically increasing static load was applied on the specimen by maintaining a suitably slow rate of deformation of the specimen until failure initiated in all specimens by bond failure within the region of anchorage length. The maximum load (P_{max}) reached at the state of bond failure in the specimen was recorded while deflection of the specimen was measured during the test utilizing LVDTs. The variables considered were the bar diameter d_b=

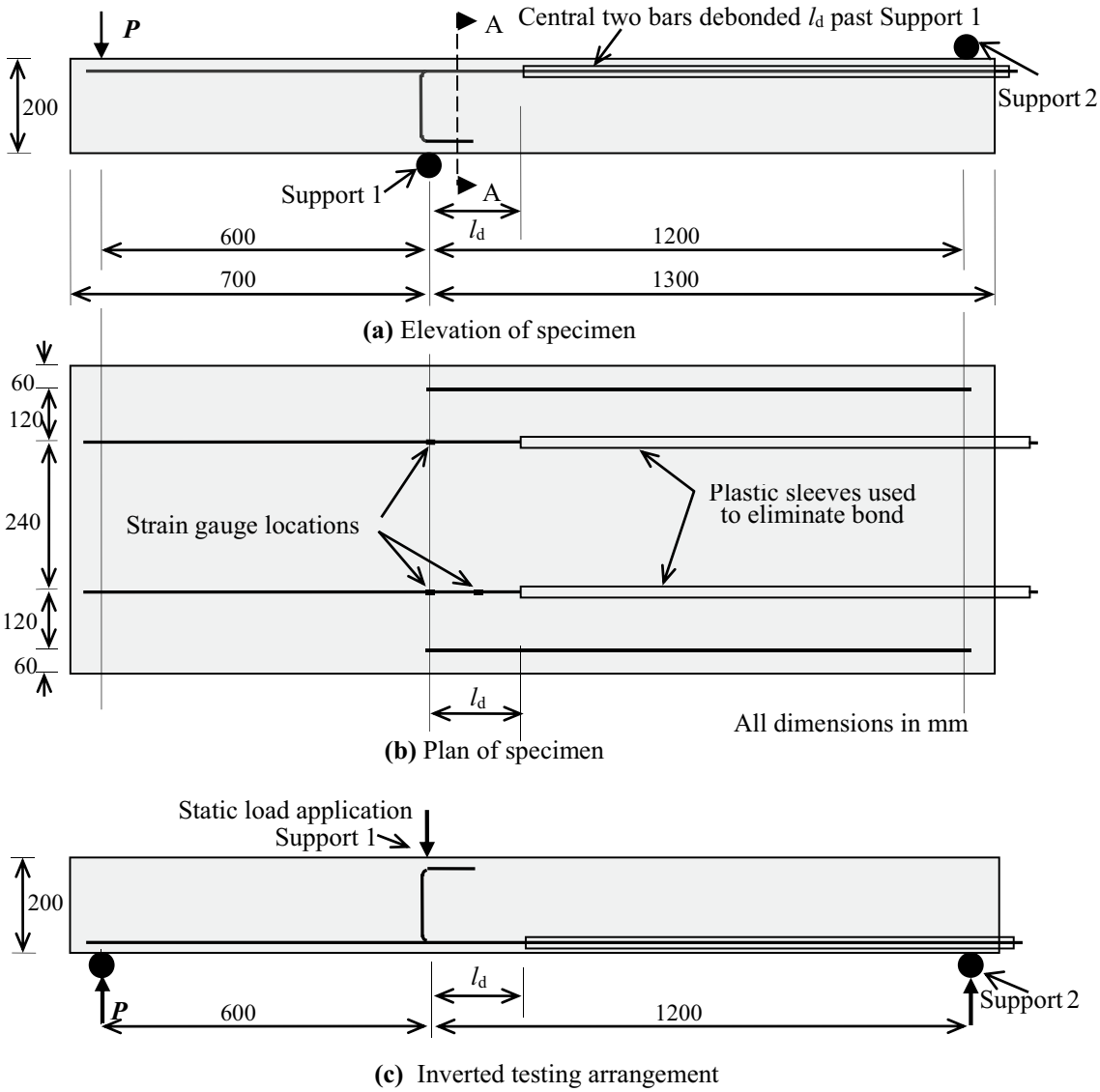

Fig. 1 Dimensions and loading arrangements of anchorage length slab specimens

12 or 16 mm; the anchorage length $l_d = 10d_b$, $15d_b$ and $20d_b$; and the bottom concrete cover $c = 25$ or 40 mm.

3 Overview of the provisions of the FIB bond–slip model

The discussion of the analytical modelling for the bond–slip behavior is made using the FIB bond–slip models [1] as a reference model as it is one of the commonly used bond–slip models for analytical and finite element (FE) modelling of RC members. The FIB model code [1] specifies local bond stress versus local slip relationships as statistical mean curves for a broad range of cases of confined and unconfined concrete. The bond stress–slip relationships applicable for two different bond failure types are defined by Eqs. (1)–(5), with constituent parameters and parametric values shown in Fig. 2; Table 1 respectively. However, these relationships are valid for short anchorage lengths only under well-defined conditions and it is recommended [1] that a designer should proceed with caution while using the FIB bond–slip models to develop design bond–slip relationships for a particular bond and anchorage problem.

For monotonic loading, the local bond stress (τ) between the concrete and reinforcing bar for pull-out and splitting bond failure can be determined as a function of the relative displacement or slip (s) according to Eqs. (1)–(4) as specified by the FIB model code [1] (notations for the equations are illustrated in Fig. 2).

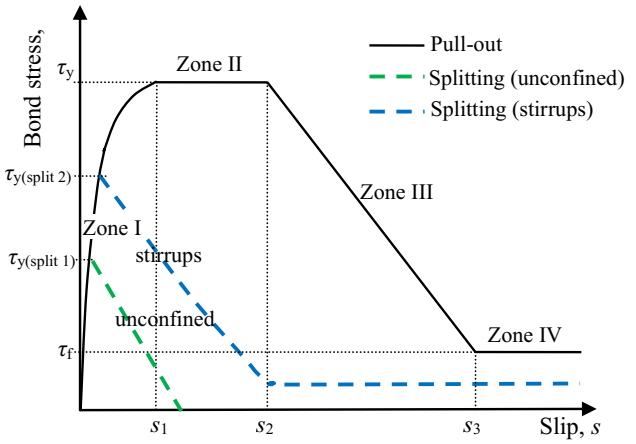

Fig. 2 Analytical bond stress–slip relationship for monotonic loading (adopted from [1])

$$\tau = \tau_y (s/s_1)^{\alpha} \text{ for } 0 \le s \le s_1. \quad (1)$$

$$\tau = \tau_y \text{ for } s_1 \le s \le s_2. \quad (2)$$

$$\tau = \tau_y - (\tau_y - \tau_f)(s - s_2)/(s_3 - s_2) \text{ for } s_2 \le s \le s_3. \quad (3)$$

$$\tau = \tau_f \text{ for } s_3 < s. \quad (4)$$

The values in Table 1 (column 2 and 3) for the pull-out type bond failure are valid for bond in well confined concrete (i.e., with $c_d \ge 5d_b$, clear spacing between bars $\ge 10d_b$). A maximum of four bond zones (Zone I–IV, as shown in Fig. 2) exist in the bond–slip relationship for the pull-out type bond failure. Two types of bond–slip relationships can be defined for the splitting type bond failure in a specific bond condition, one is for unconfined anchorage conditions in concrete ($K_{tr} = 0$) and the other is for confined anchorage conditions with stirrups. With $s_1 = s_2$, and $\tau_f = 0$ for the unconfined anchorage condition, there are two bond zones (Zone I and III, as shown in Fig. 2) in the bond–slip relationship; whereas three bond zones exist in the bond–slip relationship for the confined anchorage condition (with $s_1 = s_2$, and $\tau_f = 0.4\tau_y$). The expression for values of peak local bond stress, τ_y for the splitting type bond failures is given by Eq. (5).

$$\tau_{y(\text{split } 1,2)} = \eta_2 \cdot 6.54 \cdot (f_c'/20)^{0.25} (20/d_b)^{0.20} \left[(c_d/d_b)^{0.33} (c_{\max}/c_d)^{0.1} + 8\, K_{tr} \right], \quad (5)$$

where $\eta_2 = 1.0$ for good bond conditions and 0.7 for all other cases; f'_c is the characteristic (cylinder) compressive strength of concrete, c_{max} and c_d are the maximum and minimum available concrete cover for a bar to its nearest concrete surface, and K_{tr} is a factor that accounts for the effects of passive confinement (stirrups or transverse reinforcement). The subscript 1 at $\tau_{y(split)}$ is to denote the expression of τ_y for the splitting type bond failure in unconfined concrete ($K_{tr} = 0$) and the bond–slip relationship for unconfined anchorage condition has two bond zones as shown in Fig. 2, while the subscript 2 at $\tau_{y(split)}$ is for the expression of τ_y for the splitting bond failure in confined concrete (with a value for K_{tr}) and the bond–slip relationship for confined anchorage condition has three bond zones as shown in Fig. 2. The values of τ_y for the splitting type bond failure, given in Table 1 (column 4–7), are valid for $d_b \le 20$ mm, $c_{max}/c_d = 2.0$, $c_d = d_b$ and $K\text{tr} = 2\%$ in the case of stirrups. The factor K_{tr} is defined in the model code [1] according to Eq. (6).

$$K_{tr} = \eta_1 \cdot A_{SV}/(n \cdot d_b \cdot s_v), \quad (6)$$

where η_1 is the number of legs of confining reinforcement at a section, A_{sv} is the cross-sectional area of one leg of

Table 1 Parameters for defining mean local bond–slip relationship of deformed bars (according to [1])

Parameters (1)	Pull-out		Splitting			
	$\varepsilon_s < \varepsilon_{s,y}$		$\varepsilon_s < \varepsilon_{s,y}$			
	Good bond condition (2)	All other bond condition (3)	Good bond condition		All other bond condition	
			Unconfined (4)	Stirrups (5)	Unconfined (6)	Stirrups (7)
τ_y	$2.5\sqrt{f'_c}$	$1.25\sqrt{f'_c}$	$7.0\,(f'_c/20)^{0.25}$	$8.0\,(f'_c/20)^{0.25}$	$5.0\,(f'_c/20)^{0.25}$	$5.5\,(f'_c/20)^{0.25}$
s_1	1.0 mm	1.8 mm	$s(\tau_y)$	$s(\tau_y)$	$s(\tau_y)$	$s(\tau_y)$
s_2	2.0 mm	3.6 mm	s_1	s_1	s_1	s_1
s_3	c_{clear}*	c_{clear}*	$1.2s_1$	$0.5c_{clear}$*	$1.2s_1$	$0.5c_{clear}$*
α	0.4	0.4	0.4	0.4	0.4	0.4
τ_f	$0.40\tau_y$	$0.40\tau_y$	0	$0.40\tau_y$	0	$0.40\tau_y$

*c_{clear} (or r_b) is the clear distance between ribs

confining bar (mm^2), s_v is the longitudinal spacing of confining reinforcement (mm), n is the number of anchored bars or pairs of lapped bars, and d_b is the diameter of the anchored bar or of the smaller of the diameters of a pair of lapped bars.

4 Analytical modelling for bond–slip behavior

An example of the analytical modelling procedure that was used to calibrate bond–slip models for the anchorage of deformed bars in RC members subjected to bending is presented here. The nonlinear bond–slip relationships of the FIB model code [1] are idealized by piecewise linear curves, and are calibrated using the test results of the selected anchorage length slab specimens (denoted here as DL-1 to DL-7). The calibration [31] was done using a computationally viable analytical modelling and solution procedure that was originally proposed by Yankelevsky [32].

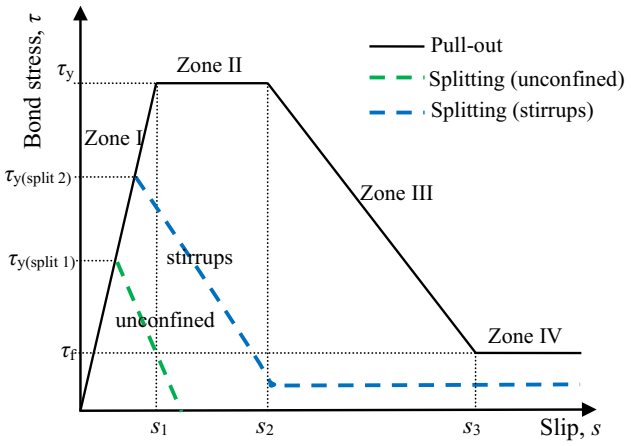

Fig. 3 Linear approximation of a typical bond–slip relationship

4.1 Mathematical formulations of analytical modelling

With minor changes in the mathematical formulations of local bond stress, τ (x) and slip, s(x) for the bond–slip relationship in bond zone III, the analytical model [32] used for modelling bond–slip behavior is outline below. The nonlinear bond stress–slip relationships are idealized by linear relationships in up to four possible bond zones (Fig. 3) and second-order linear differential equations for the different bond zones are defined. The boundary conditions are the strains in the reinforcing bar $\varepsilon_s(x)$ at the two ends of the anchorage length (l_d):

$$\text{at } x = 0 : \varepsilon_s(x) = 0 \text{at } x = l_d : \varepsilon_s(x) = \varepsilon_0,$$

where ε_o is the strain calculated from the bar stress, σ_{st} (at P_{max}), based on the analysis of the cracked section at $x = l_d$.

Depending on the given boundary conditions and satisfying conditions of compatibility at the interface of the bond zones, the differential equations can be solved for any appropriate bond–slip relationship to find the unknown lengths of the bond zones within the anchorage length (e.g., Fig. 4) of an anchorage specimen. A detail description of mathematical formulations and solutions of the analytical model is outline below.

The formulation of typical analytical and numerical models for bond–slip in reinforced concrete is based upon the assumption that the influence of concrete deformation on slip is negligible especially when bond failure occurs with the strain in the reinforcing bar below the yield strain [32]. Hence, the strain in the bar is related to the slip by:

$$\varepsilon_s(x) = \frac{ds(x)}{dx} \tag{7}$$

Equilibrium of an infinitesimal bar element at distance x, yields the relationship between the bond stress $\tau(x)$ and the axial force $T_s(x)$ in the steel bar:

$$\tau(x) = \frac{1}{\pi d_b}\frac{dT_s(x)}{dx} \tag{8}$$

Assuming linear-elastic behavior of the steel bar:

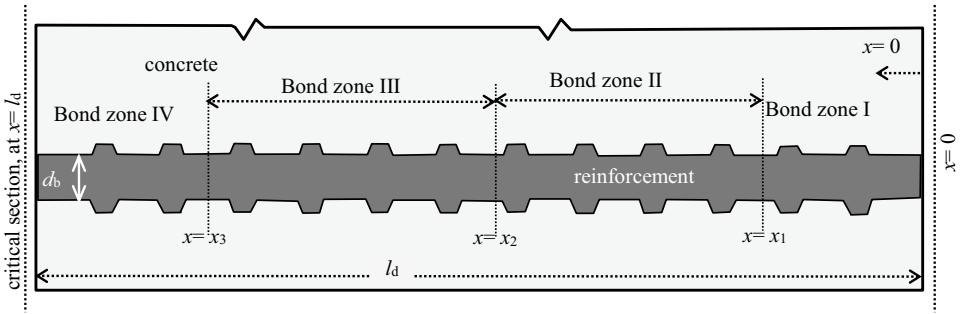

Fig. 4 Idealization of bond zones within the anchorage (for typical pull-out bond failure)

$$\tau(x) = \frac{E_s A_s}{\pi d_b} \frac{d\varepsilon_s(x)}{dx} \tag{9}$$

in which E_s and A_s are the Young's modulus of elasticity and the cross-sectional area of the reinforcing bar, respectively. Substituting Eqs. (7) into (9), when a circular cross-section of the bar is assumed, we get:

$$\tau(x) = \frac{E_s d_b}{4} \frac{d^2 s(x)}{dx^2} \tag{10}$$

The solutions of the differential equation yields the expressions for slip, strain and bond stress variations within a particular bond zone and the mathematical expressions for the solutions are presented below.

(a) Zone I: $0 \le s(x) \le s_1$

The variation of bond stress with slip is:

$$\tau(x) = K_y s(x) \tag{11}$$

where $K_y = \tau_y / s_1$. Substituting Eqs. (11) into (10) yields:

$$\frac{d^2 s(x)}{dx^2} - \frac{4K_y}{E_s d_b} s(x) = 0 \tag{12}$$

and solving gives:

$$s(x) = C_1 e^{\alpha_1 x} + C_2 e^{-\alpha_1 x} \tag{13}$$

where $\alpha_1 = \sqrt{4K_y / E_s d_b}$ and C_1 and C_2 are constants to be determined from the known boundary conditions.

The expression for strain variation becomes:

$$\varepsilon_s(x) = \frac{ds(x)}{dx} = \alpha_1 \left[C_1 e^{\alpha_1 x} - C_2 e^{-\alpha_1 x}\right] \tag{14}$$

(b) Zone II: $s_1 \le s(x) \le s_2$

The expression for bond stress in this zone is:

$$\tau(x) = \tau_y \tag{15}$$

Substituting Eqs. (15) into (10) yields:

$$\frac{d^2 s(x)}{dx^2} = \frac{4\tau_y}{E_s d_b} \tag{16}$$

and solving gives:

$$s(x) = \frac{2\tau_y}{E_s d_b} x^2 + C_3 x + C_4 \tag{17}$$

where C_3 and C_4 are constants to be determined from the known boundary conditions.

The expression for strain variation is:

$$\varepsilon_s(x) = \frac{ds(x)}{dx} = \frac{4\tau_y}{E_s d_b} x + C_3 \tag{18}$$

(c) Zone III: $s_2 \le s(x) \le s_3$

The expression for bond stress in this zone is:

$$\tau(x) = \tau_y - K_2 [s(x) - s_2] \tag{19}$$

in which:

$$K_2 = \frac{\tau_y - \tau_f}{s_3 - s_2} \tag{20}$$

Substituting Eqs. (19) into (10) yields:

$$\frac{d^2 s(x)}{dx^2} + \frac{4K_2}{E_s d_b} s(x) = \frac{4\tau_y}{E_s d_b} + \frac{4K_2 s_2}{E_s d_b} \tag{21}$$

and solving gives:

$$s(x) = C_5 \sin(\alpha_2 x) + C_6 \cos(\alpha_2 x) + \frac{\tau_y}{K_2} + s_2 \tag{22}$$

where $\alpha_2 = \sqrt{4K_2 / E_s d_b}$ and C_5 and C_6 are constants to be determined from the known boundary conditions. The expression for strain variation in the steel bar becomes:

$$\varepsilon_s(x) = \frac{ds(x)}{dx} = \alpha_2 \left[C_5 \cos(\alpha_2 x) - C_6 \sin(\alpha_2 x)\right] \tag{23}$$

(d) Zone IV: $s_3 \le s(x)$.

In this zone there exists a constant bond stress

$$\tau(x) = \tau_f \tag{24}$$

Similarly to Zone II, where the bond stress is also uniform, the expressions for slip and strain are:

$$s(x) = \frac{2\tau_f}{E_s d_b} x^2 + C_7 x + C_8 \tag{25}$$

$$\varepsilon_s(x) = \frac{4\tau_f}{E_s d_b} x + C_7 \tag{26}$$

With four distinct bond zones (Fig. 4) along the length of an anchored bar for the pull-out type bond failure, a maximum of 11 unknowns (eight constants C_1 to C_8 and three values for x (i.e. x_1, x_2, x_3) exist in the formulation and are required for the solution. These unknowns may be determined by an analytical solution procedure or using optimization algorithm for solution [31] with input values satisfying the boundary conditions and the conditions of compatibility as follows:

- At each of the three common boundaries between the four zones, the conditions of compatibility (equality) between bond stresses, slip and strain.
- At $x = l_d$, and at $x = 0$, the strain in the bar is known.

4.2 Calibration of bond–slip models for selected anchorage length specimens

An example of the procedure followed for calibrating bond–slip models using the test results of the selected anchorage length RC slab specimens (denoted as DL-1 to DL-7) is presented here. The anchored bars within each specimen were unconfined and splitting type bond failure was observed in all the specimens under overload. Therefore, according to the FIB model code [1], it is reasonable to assume that bond–slip relationship with two bond zones (bond zone I and III) controlled the bond–slip behavior in the selected specimens. Referring to Fig. 3, when bond failure occurs under the maximum applied load, at one location within the anchorage of the specimen the bond stress τ reaches τ_y with a local slip s_1. In this case, with no zone II ($s_1 = s_2$) existing in the bond–slip relationship, compatibility of strains, slips and bond stresses must exist at the point of transition between the two bond zones I and III. Bond zone III continues up to the point where $\tau_f = 0$ and $s = s_3$. In this case, with no s_4, zone IV also does not exist. Figure 5 shows the idealization of the bond zones as assumed within the anchorage length of each selected specimen.

The boundary values of strains at the two ends of the anchorage length (l_d) are calculated by cracked section analysis from the experimental test results. Using the input boundary values and compatibility conditions in the analytical solution, a total of four unknowns exist (unknown bond zone I length x_1, as well as constants C_1, C_5 and C_6) and these can be solved in a trial and error method using a bond–slip relationship appropriate for a specimen. The mathematical formulations and solution procedure outlined in Sect. 4.1 is used to determine the value of the unknowns (length of bond zone I, x_1; value of constants C_1, C_5 and C_6). The known boundary and compatibility conditions used for the solutions are:

At $x = l_d$, $\varepsilon(x) = \varepsilon_0$, ($\varepsilon_0$ determined from P_{max}, by cracked section analysis),

At $x = 0$, $\varepsilon(x) = 0$,

Bond stress, strain and slip are equal at the transition between the two bond zones, $\tau_I(x_1) = \tau_{III}(x_1) = \tau_y$, $s_I(x_1) = s_{III}(x_1) = s_1 = s_2$,

According to the solution procedure, Eqs. (27)–(30) provides solutions for each of the unknowns C_1, C_5, C_6 and x_1 for the two bond zone conditions (Zone I and III) existing in the bond–slip models for the selected specimens:

$$C_1 = C_2 = \frac{s_1}{2\cosh(\alpha_1 x_1)} \tag{27}$$

$$C_5 = \frac{\varepsilon_{so} + \alpha_2 C_6 \sin(\alpha_2 l_d)}{\alpha_2 \cos(\alpha_2 l_d)} \tag{28}$$

$$C_6 = \frac{\alpha_2 C_5 \cos(\alpha_2 x_1) - 2\alpha_2 C_1 \sinh(\alpha_1 x_1)}{\alpha_2 \sin(\alpha_2 x_1)} \tag{29}$$

$$x_1 = \sin^{-1} \frac{\left(\frac{-\frac{\tau_y}{K_2} - C_6 \cos(\alpha_2 x_1)}{C_5} \right)}{\alpha_2} \tag{30}$$

The system of equations can be solved by manual calculations or using optimization algorithm for solution [31] with given input values of respective material parameters, boundary conditions of strains, constituent parameters of the bond–slip relationship, length of the anchorage (l_d) and assumed initial values of unknowns. The bond–slip relationships as specified according to the FIB model code [1] for splitting bond failure were first used to check the solutions of the unknown length of bond zones for the selected specimens. Table 2 shows the bond–slip relationships for the specimens, as specified according to the FIB model code. The structural and material parameters of the specimens are also shown in the table. With the bond–slip relationships of the FIB model code, i.e. with the values of s_1, s_3 and τ_y given in Table 2, no practical solutions of the unknown bond zone lengths ($x_1 < l_d$) could be found for the selected specimens

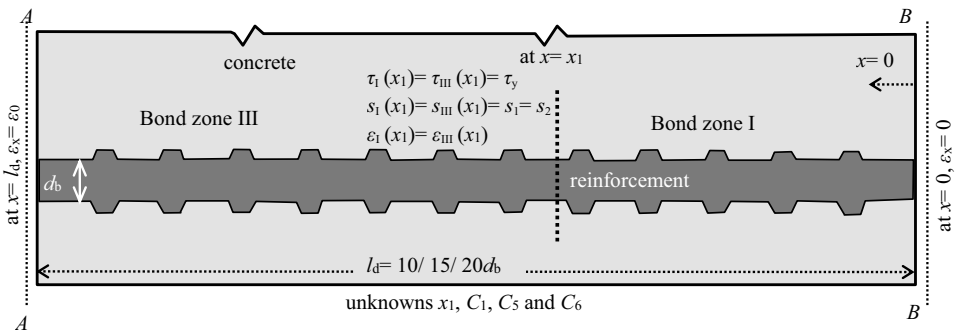

Fig. 5 Idealization of bond zones within the anchorage of the selected specimens

Table 2 Parameters of bond–slip relationships for the selected specimens (specified according to the FIB Model Code 2010 [1])

Parameters	Splitting type bond failure (good bond condition and unconfined anchorage condition) $\varepsilon_s < \varepsilon_{s,y}$		
	DL-1, 2	DL-3 to 5	DL-6, 7
τ_y (MPa)	10.19	11.86	11.23
s_1 (mm)	0.35	0.51	0.47
s_2 (mm)	0.35	0.51	0.47
s_3 (mm)	0.42	0.61	0.56
α	0.4	0.4	0.4
τ_f	0	0	0
Structural and material parameters	d_b= 16 mm, c_d= 25 mm, c_{max}= 60 mm, f'_c= 38.5 MPa, f_{sy}= 546 MPa	d_b= 12 mm, c_d= 25 mm, c_{max}= 60 mm, f'_c= 38.5 MPa, f_{sy}= 561 MPa	d_b= 16 mm, c_d= 40 mm, c_{max}= 60 mm, f'_c= 36.9 MPa, f_{sy}= 546 MPa

except for the specimen DL-1. However, real solutions of the unknown bond zone lengths for the seven selected anchorage length specimens could be determined using a revised bond–slip relationship with constituent parameters reasonably estimated from measurements made in the experimental program. The experimentally measured end-slip of the debonded bars at P_{max} was used to decide reasonable initial values of the parameter s_1/s_2, and the post-peak end slip of the bars at $0.4P_{max}$ gave an indication of the spread of the tail end of the bond slip relationship (s_3).

Since more than one set of real solutions of unknowns for a specimen could be determined for different sets of parameters for the bond–slip relationships, further analyses were performed to calculate the local bond stresses at locations of the ribs of the reinforcement within the anchorage length of each specimen. The average of the calculated local bond stresses ($\tau_{avg,cal}$) along the anchored bar of a specimen was compared for consistency with the experimentally determined average bond stress ($\tau_{avg,exp}$ at P_{max}) for that specimen. In a trial and error procedure, the bond–slip relationship was adjusted and the analytical solution procedure was repeated until the $\tau_{avg,cal}$ and $\tau_{avg,exp}$ agreed well. Trial and error calculations of the analytical solutions for local bond stresses and subsequently for checking consistency between $\tau_{avg,cal}$ and $\tau_{avg,exp}$ can be done using a simple and convenient programming routine (e.g., [31]).

In this way, the constituent parameters of the calibrated bond–slip relationships determined for two of the test specimens are shown in Figs. 6 and 7 respectively for DL-1 and DL-2, from which the real solutions of the unknown length of the bond zones (x_1) could be determined (as shown in the figures) while the $\tau_{avg,cal}$ also agreed reasonably well with measured $\tau_{avg,exp}$ for each specimen. The calibrated bond–slip relationships for the seven selected specimens as determined according to this procedure is shown in Table 3.

The limitation of the typical analytical modelling procedure is that the effect of concrete deformation on bond stresses is neglected, as is commonly assumed when $\varepsilon_s < \varepsilon_{s,y}$. If in fact there was no influence of concrete deformation on bond stress, the average bond stresses would be the same for

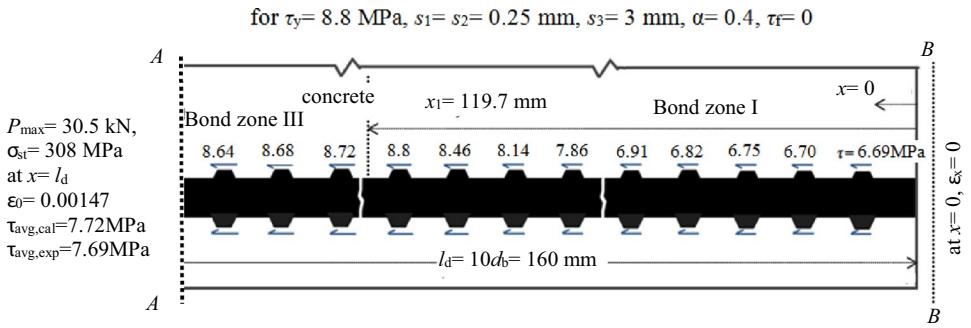

Fig. 6 Bond zone length and local bond stresses determined by calibrated bond–slip relationship for DL-1

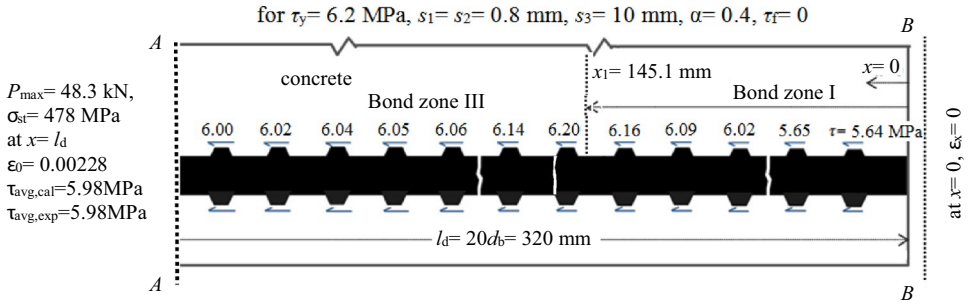

Fig. 7 Bond zone length and local bond stresses determined by calibrated bond–slip relationship for DL-2

Table 3 Calibrated parameters of the bond–slip relationships for selected anchorage length specimens and results of analytical modelling

Specimens (bond–slip relationships)	Constitutive parameters of the bond–slip relationships (unconfined, good bond condition)$\varepsilon_s < \varepsilon_{s,y}$						Bond zone I length (x_1) (mm)	Average bond stress within anchorageτ_{avg} (MPa)	Structural and material parameters
	τ_y(MPa)	s_1 (mm)	s_2 (mm)	s_3 (mm)	α	τ_f(MPa)			
DL-1, l_d= $10d_b$ = 160 mm (calibrated)	8.80	0.25	0.25	3	0.4	0	119.7	$\tau_{avg,exp}=7.69\tau_{avg,cal}=7.72$	d_b= 16 mm, c = 25 mm, c_{max}= 60 mm, f'_c= 38.5 MPa, f_{sy}= 546 MPa
DL-2, l_d= $20d_b$ = 320 mm (calibrated)	6.20	0.8	0.8	10(*≈c_r)	0.4	0	145.1	$\tau_{avg,exp}=5.98\tau_{avg,cal}=5.98$	
DL-1, 2 (FIB bond–slip model)	10.19	0.35	0.35	0.42	0.4	0	107.2(DL-1)	$\tau_{avg,exp}=7.69\tau_{avg,cal}=7.51$(DL-1)	
DL-3, l_d= $10d_b$ = 120 mm (calibrated)	12.80	0.40	0.40	4	0.4	0	80.9	$\tau_{avg,exp}=11.92\tau_{avg,cal}=11.90$	d_b= 12 mm, c = 25 mm, c_{max}= 60 mm, f'_c= 38.5 MPa, f_{sy}= 561 MPa
DL-4, l_d= $15d_b$ = 180 mm (calibrated)	10.40	0.6	0.6	6	0.4	0	132.3	$\tau_{avg,exp}=9.41\tau_{avg,cal}=9.35$	
DL-5, l_d= $20d_b$ = 240 mm (calibrated)	9.00	0.7	0.7	7(*≈c_r)	0.4	0	234.8	$\tau_{avg,exp}=6.72\tau_{avg,cal}=6.72$	
DL-3 to 5 (FIB bond–slip model)	11.86	0.51	0.51	0.61	0.4	0	No real solution	–	
DL-6, l_d= $10d_b$ = 160 mm (calibrated)	10.00	0.25	0.25	3	0.4	0	159.1	$\tau_{avg,exp}=7.31\tau_{avg,cal}=7.42$	d_b= 16 mm, c = 40 mm, c_{max}= 60 mm, f'_c= 36.9 MPa, f_{sy}= 546 MPa
DL-7, l_d= $20d_b$ = 320 mm (calibrated)	7.00	0.80	0.80	10(*≈c_r)	0.4	0	252.3	$\tau_{avg,exp}=6.02\tau_{avg,cal}=6.03$	
DL-6, 7 (FIB bond–slip model)	11.23	0.47	0.47	0.56	0.4	0	No real solution	–	

*c_r (or r_b) is the rib spacing

identical specimens (where the same materials are used in the same structural geometry) regardless of the variation of anchorage lengths. The bond–slip relationships according to the FIB design model for the identical anchorage length specimens (e.g. DL-1, DL-2) are, in fact, the same regardless of the variations of the anchorage lengths. However, Table 3 shows that the constituent parameters of the recalibrated bond–slip relationships are, in fact, different for variations of anchorage lengths in otherwise identical specimens. Therefore, the changes of the constitutive parameters of the calibrated bond–slip relationships for each specimen indirectly accounts for the effect of concrete deformation on bond stresses. Table 3 also shows that the constituent parameters of some of the calibrated bond–slip relationships are significantly different when compared to the FIB bond–slip relationships for the respective specimens (e.g. for DL-2, DL-5, DL-6 and DL-7), both in terms of peak local bond stress, τ_y and constituent local slip values in different bond zones.

4.3 Modified model for peak local bond stress of the bond–slip model

The analyses presented in this section are aimed at developing a modified general model of the peak local bond stress ($\tau_{y(split)}$) for splitting type bond failure, that is applicable for both the unconfined and confined anchorage conditions in

RC members in bending. The modified model for $\tau_{y(split)}$ of the bond–slip relationship is developed for best consistency with the respective calibrated values of $\tau_{y(split)/cal}$ for all the seven selected specimens.

The bond–slip model of the FIB model code [1] for splitting type bond failure considers the effects of variations of the bar diameter, the concrete strength and the concrete cover on the mean local bond stresses of the bond–slip model. The FIB model Eq. (1) is specified according to Eq. (31) to determine peak local bond stress $\tau_{y(split)}$ (either $\tau_{y(split)0.1}$ or $\tau_{y(split)0.2}$) for the splitting type bond failure.

$$\tau_{y(split\ 1,2)} = \eta_2 k_1 \left(\frac{f'_c}{20}\right)^{0.25} \left(\frac{20}{d_b}\right)^{k_2} \left[\left(\frac{c_d}{d_b}\right)^{k_4} \left(\frac{c_{max}}{c_d}\right)^{0.1} + 8K_{tr}\right] \tag{31}$$

where $k_1 = 6.54$, $k_2 = 0.20$, $k_4 = 0.33$ [as also shown in Eq. (5)].

The modified model will also include the effect of the anchorage length on the magnitude of $\tau_{y(split)}$. It additionally includes a factor $(20d_b/l_d)$ with exponent k_3 which is newly introduced to account for the effect of the variation of anchorage lengths on peak local bond stress $\tau_{y(split)}$ (either $\tau_{y(split)0.1}$ or $\tau_{y(split)0.2}$) for the splitting type bond failure. The modified model for $\tau_{y(split\ 1,2)}$ now becomes

$$\tau_{y(split\ 1,2)} = \eta_2 k_1 \left(\frac{f'_c}{20}\right)^{0.25} \left(\frac{20}{d_b}\right)^{k_2} \left(\frac{20d_b}{l_d}\right)^{k_3} \left[\left(\frac{c_d}{d_b}\right)^{k_4} \left(\frac{c_{max}}{c_d}\right)^{0.1} + 8K_{tr}\right] \tag{32}$$

An optimization function was solved to determine unknown values of coefficients of Eq. (32) [31]. The optimization routine gave outputs of best combination of the values of the coefficients k_1, k_2, k_3 and k_4 in Eq. (32) that optimally minimized differences between f(DL) and respective $\tau_{y(split)/cal}$(DL), where f (DL) represents set of values of $\tau_{y(split)}$ for the selected specimens determined according to Eq. (32) and $\tau_{y(split)/cal}$(DL) represents the calibrated values of $\tau_{y(split)}$ for the specimens as shown in Table 3. Hence, the optimized values of the factors are determined as $k_1 = 3.3$, $k_2 = 0.9$, $k_3 = 0.5$ and $k_4 = 0.4$. The modified model of $\tau_{y(split)}$ for splitting type bond failure is written in Eq. (33). The average difference between the calculated values of $\tau_{y(split)}$ (according to Eq. 33) and that of the calibrated bond–slip relationship for the selected specimens is 0.9%.

$$\tau_{y(split\ 1,2)} = 3.33\eta_2 \left(\frac{f'_c}{20}\right)^{0.25} \left(\frac{20}{d_b}\right)^{0.9} \left(\frac{20d_b}{l_d}\right)^{0.5} \left[\left(\frac{c_d}{d_b}\right)^{0.4} \left(\frac{c_{max}}{c_d}\right)^{0.1} + 8K_{tr}\right] \tag{33}$$

The modified model (Eq. 33) for estimating peak local bond stress $\tau_{y(split)}$ was successfully verified [31] in calibrating bonds–slip models for several full-scale RC beam specimens tested in bending where lapped splices of reinforcement were provided in the specimens under different confinement conditions (with specified K_{tr}).

5 Conclusions

The procedure for recalibration of bond–slip relationships for the anchorage of deformed bars as presented in this paper is based on observations of load–deflection behavior in laboratory experiments of a few selected full-scale RC anchorage specimens subjected to bending. The RC specimens were designed with relatively long end development of anchorage bars beyond a critical section. The specimens were tested under the application of monotonic static load which showed typical splitting type bond failure within the anchorage zone. The major finding of the experimental study was that the concrete deformation had a significant effect on bond stresses, especially when longer anchorages were provided in full-size RC specimens.

A simple but computationally viable analytical modelling procedure is used for calibrating bond–slip models for the anchorage of deformed bars in the RC members under bending. The constituent parameters of the bond–slip models recalibrated based on the test results of the RC anchorage length slab specimens show significant variations of mean local bond stresses and of local slip values when compared with the FIB model specifications of bond–slip relationships for the respective specimens. The variations of the calibrated bond–slip models depending on the variations of anchorage lengths in otherwise identical specimens indirectly account for the influences of concrete deformation on bond stresses.

A modified model for estimating peak local bond stress of the bond–slip model is also presented in this paper. The modified model proposed in the paper takes into account the effect of variations of anchorage length on the peak local bond stress, in addition to the effects of bar diameters, concrete cover and concrete strength that are typically accounted for in the model codes or specifications. However, the application of the bond–slip models presented in this paper should be limited for modelling short but practical anchorage lengths ($l_d \leq 20d_b$ with $d_b \leq 20$ mm) where splitting type bond failure is expected to occur within the anchorage length of RC members under bending.

Acknowledgements The experimental work of the research project (PhD) was undertaken at the University of New South Wales, Sydney, Australia with the financial support of the Australian Research Council (ARC) through an ARC Discovery (DP1096560) grant to the second author. This support is gratefully acknowledged.

Declarations

Conflict of interest On behalf of all authors, the corresponding author states that there is no conflict of interest.

References

1. FIB (2012) Model Code 2010: final draft FIB MC-10: 2012. International Federation for Structural Concrete, Lausanne
2. Standards A (2018) AS 3600:2018-Australian Standard for Concrete Structures, BD-002: concrete structures. Standards Australia, Sydney
3. ACI (2014) ACI 318–14: building code requirements for structural and commentary. ACI Committee 318. American Concrete Institute, Indiana
4. CEN (2004) BS-EN-1992-1-1:2004 - Eurocode 2: Design of Concrete Structures Part 1–1: General Rules and Rules for Buildings. European Committee for Standardization, Brussels
5. DIN (2008) DIN 1045-1: concrete, reinforced and prestressed concrete structures-part 1: design and construction. Deutsches Institut für Normung, Berlin
6. Comité Euro-International du Béton (1983) RILEM-CEB-FIP-RC6 recommendation RC 6: bond test reinforcement steel. 2. Pull-out test. Concrete Reinforcement Technology, Paris
7. Comité Euro-International du Béton (1982) RILEM-CEB-FIP-RC 5: bond test for reinforcement steel. 1. Beam test. Concrete Reinforcement Technology, Paris
8. Cairns J (2015) Bond and anchorage of embedded steel reinforcement in *fib* model code 2010. Struct Concr 16(1):45–55
9. Cairns J (2021) Local bond-slip model for plain surface reinforcement. Struct Concr 22(2):666–675
10. Mazumder MH, Gilbert RI, Chang ZT (2020) Anchorage length of reinforcing bars in tension: an assessment of the Australian Standard AS 3600:2018. Asian J Civ Eng 21(3):411–420
11. Mousavi SS, Mousavi Ajarostaghi SS, Bhojaraju C (2020) A critical review of the effect of concrete composition on rebar-concrete interface (RCI) bond strength: a case study of nanoparticles. SN Appl Sci 2:893. https://doi.org/10.1007/s42452-020-2681-8
12. Mang C, Jason L, Davenne L (2015) A new bond slip model for reinforced concrete structures: validation by modelling a reinforced concrete tie. Eng Comput 32(7):1934–1958
13. Ghavamian S, Carol I, Delaplace A (2003) Discussions over MECA project results. Revue Française de Génie Civil 7(5):543–581
14. Parmar RM, Signh T, Thangamani I, Trivedi N, Singh RK (2014) Over-pressure test on BARCOM pre-stressed concrete containment. Nucl Eng Des 269:177–183
15. Mazumder MH, Gilbert RI (2019) Finite element modelling of bond-slip at anchorages of reinforced concrete members subjected to bending. SN Appl Sci 1:1332. https://doi.org/10.1007/s42452-019-1368-5
16. Gilbert RI, Mazumder MH, Chang ZT (2012) Bond, slip and cracking within the anchorage length of deformed reinforcing bars in tension. In: Proceedings of international conference of the bond in concrete BIC-2012, Brescia, Italy
17. Kilpatrick AE, Gilbert RI (2012) A preliminary investigation of the strength and ductility of lapped splices of reinforcing bars in tension. In: Proceedings of 22nd Australasian conference on the mechanics of structures and materials ACMSM 22, CRC Press, CPI Group (UK) Ltd, Croydon, pp 305–311, presented at the 22nd ACMSM, 11–14 December 2012, Sydney, Australia
18. Jason L, Torre-Casanova A, Davenne L, Pinelli X (2013) Cracking behavior of reinforced concrete beams: experiment and simulations on the numerical influence of the steel-concrete bond. Int J Fract 180:243–260. https://doi.org/10.1007/s10704-013-9815-6
19. Gambarova P, Balazs G, Vliet AB, Cairns J, Eligehausen R, Engstrom B, Giuriani E, Leon R, Mayer U, McCabe S, Noghabai K, Plizzari G, Rosati GP, Russo G, Shima H, Ueda T, Vandewalle L (2000) Bond mechanics including pull-out and splitting failures, In: Chap. 1 of State-of-Art report on 'bond of reinforcement in concrete', *fib* Bulletin No. 10 edited by *fib* Task Group "bond models" chaired by Tepfers R, pp 1–98
20. Eligehausen R, Popov EP, Bertoro VV (1982) Hysteretic behavior of reinforcing deformed hooked bars in reinforced concrete joints. In: Proceedings of the 7th European conference of earthquake engineering, vol 4, 20–25 September 1982, Athens, Greece, pp 171–178
21. Alsiwat JM, Saatcioglu M (1992) Reinforcement anchorage slip under monotonic loading. ASCE J Struct Eng 118(9):2421–2438
22. Bigaj AJ (1999) Structural dependence of rotation capacity of plastic hinges in RC beams and slabs. PhD thesis, Delft University of Technology, Netherlands **(ISBN 90-407-1926-8)**
23. Lehman DE, Moehle JP (2000) Seismic performance of well-confined concrete bridge columns. In: Report PEER-1998/01. Pacific Earthquake Engineering Research Center, University of California, Berkeley
24. Sezen H, Moehle JP (2003) Bond-slip behavior of reinforced concrete members. In: Proceedings of the *fib* symposium on concrete structures in seismic regions, CEB-FIP, Athens, Greece
25. Lundgren K, Magnusson J (2001) Three-dimensional modelling of anchorage zones in reinforced concrete. J Eng Mech 127(7):693–699
26. Gilbert RI, Chang ZT, Mazumder MH (2011) Anchorage of reinforcement in concrete structures subjected to cyclic loading. In: Proceedings of 25th Biennial conference of concrete Institute of Australia Concrete-11, Perth, Australia
27. Mazumder MH, Gilbert RI, Chang ZT (2012a) Bond and anchorage length of deformed bars in tension: way forward for advanced formulations. In: Proceedings of international conference AARCV 2012, Kerala, India, pp 154–161
28. Mazumder MH, Gilbert RI, Chang ZT (2012) A reassessment of the analysis provisions for bond and anchorage length of deformed reinforcing bars in tension. Bonfring Int J Ind Eng Manag Sci 2(4):01–08
29. Mazumder MH, Gilbert RI, Chang ZT (2013a) Anchorage of deformed reinforcing bars in tension: an outlook for advanced formulation of a bond-slip constitutive relationship. In: Proceedings of 22nd Australasian conference on the mechanics of structures and materials ACMSM 22, CRC Press, CPI Group (UK) Ltd, Croydon, pp 319–324, presented at the 22nd ACMSM, 11–14 December 2012, Sydney, Australia
30. Mazumder MH, Gilbert RI, Chang ZT (2013b) Analytical modelling of average bond stress within the anchorage of tensile reinforcing bars in reinforced concrete members. WASET Int J Civ Environ Eng 7(6):392–398
31. Mazumder MH (2014) The anchorage of deformed bars in reinforced concrete members subjected to bending. PhD thesis, University of New South Wales, Kensington, NSW, Australia
32. Yanakelevsky DZ (1985) Analytical model for bond-slip behavior under monotonic loading. Build Environ 20(3):163–168